Use of laterite as a sustainable catalyst for removal of fluoroquinolone antibiotics from contaminated water

M. Kamagaté, A.A. Assadi, T. Kone, S. Giraudet, L. Coulibaly, K. Hanna

Use of laterite as a sustainable catalyst for removal of fluoroquinolone antibiotics from contaminated water

Mahamadou Kamagate[1 2], Aymen Amin Assadi [1], Tiangoua Kone [2], Sylvain Giraudet[1], Lacina Coulibaly[2], Khalil Hanna[1]*

[1]Ecole Nationale Supérieure de Chimie de Rennes, UMR CNRS 6226, 11 Allée de Beaulieu, F-35708 Rennes Cedex 7, France

[2]Université Nangui Abrogoua, 02 BP 801 Abidjan 02, Côte d'Ivoire.

*Corresponding author. Tel: +33(0)223238027, Fax: +33(0)223238120, E-mail: khalil.hanna@ensc-rennes.fr

Abstract

Although there is a growing interest in Fenton oxidation processes based on natural catalysts, the use of laterite soil to promote sequential adsorption/oxidation treatments of fluoroquinolone antibiotics has been scarcely investigated. In this work, the ability of an african laterite containing goethite and hematite to remove flumequine (FLU), used as a representative compound of fluoroquinolone antibiotics, was evaluated under dark and UVA irradiation. Batch experiments and liquid chromatography analyses showed that the presence of laterite can enhance FLU removal from heavily contaminated water through both sorption and oxidation reactions (up to 94% removal of 77 µmol L^{-1} of FLU and 72% of mineralization). The heterogeneous reaction rate is dominated by the rate of intrinsic surface chemical reactions including sorption and oxidation of FLU, and light-induced reduction of Fe^{III} sites to produce Fe^{II}. Based on the probe and scavenging experiments, $^{\bullet}OH$ radicals were mainly involved in the heterogeneous oxidation reaction. The photo-assisted Fenton process showed a high efficiency of FLU removal even in the presence of a second fluoroquinolone antibiotic, norfloxacin (NOR), which can be co-found with FLU in affected environments. Determinations of kinetic rate constants and total organic carbon (TOC) for five sequential adsorption/oxidation cycles showed that laterite exhibited no deactivation of surface sites and an excellent catalytic stability. This cost-effective and environmentally friendly remediation technology may appear as a promising way for the removal of fluoroquinolone antibiotics from multi-contaminated waters.

Keywords: Laterite; fluoroquinolone antibiotics; sorption; oxidation; stability; UVA irradiation.

1. Introduction

Fenton reaction based on generation of highly reactive oxygen species (ROS) has attracted continuous attention during the past decades, and is considered as a powerful oxidative method for the treatment of persistent organic pollutants (Anipsitakis and Dionysiou 2004; Pignatello et al. 2006). In homogeneous Fenton process, dissolved iron and H_2O_2 are used to produce ROS (Anipsitakis and Dionysiou 2004; Pignatello et al. 2006). In heterogeneous system, iron oxy-hydroxides, iron bearing minerals and/or iron immobilized diverse supports are generally used to promote the Fenton reaction (Lin and Gurol 1998; Kwan and Voelker 2003; Matta et al. 2007; Gonzalez-Olmos et al. 2009; Guo et al. 2010; Ghauch et al. 2011; Gonzalez-Olmos et al. 2012; Wang et al. 2015; Lan et al. 2015). The latter process offers many advantages over its homogeneous counterpart, such as no sludge formation, operation at near neutral pH, easy separation/recovery of catalyst, etc. (Martínez et al. 2007 ; Gonzalez-Olmos et al. 2009; Guo et al. 2010; Herney-Ramirez et al. 2010 ; Gonzalez-Olmos et al. 2012; Minella et al. 2014). Because the decomposition rate of organic contaminants in heterogeneous system is slower than in classic homogeneous Fenton reaction, different ways have been developed to enhance the oxidation efficiency while keeping the benefits of heterogeneous system. Among these processes, the photo-assisted Fenton reaction using light energy can accelerate the reaction rate by decomposing H_2O_2 into most powerful oxidizing species, and by reducing Fe^{III} to Fe^{II} and/or converting Fe^{III} back to Fe^{II} after the reaction (Martínez et al. 2007 ; Herney-Ramirez et al. 2010 ; Gonzalez-Olmos et al. 2012; Minella et al. 2014).

Different synthetic materials have been used as a catalyst in heterogeneous Fenton processes, e.g. iron oxides (Matta et al. 2007; Minella et al. 2014; Wang et al. 2015), zeolite (Gonzalez-Olmos et al. 2009; 2012), clay (Bohu et al. 2008; Herney-Ramirez et al. 2010), and modified iron-carbon (Lan et al. 2015). However, the use of these materials for high-scale applications

76 in water and wastewater treatment may be limited due to their low effectiveness and/or high
77 costs (Garrido-Ramirez et al. 2010; Litter et al. 2017). Indeed, the high cost of supported or
78 composite catalysts leads the researchers to propose a cheaper alternative, particularly in the
79 developing countries.
80 Laterite soil is abundant in some parts of the earth including Africa. Although some studies
81 were dedicated to the use of laterite in Fenton reactions (Karale et al. 2013; Khataee et al.
82 2015), much remains to be learned on the sorption/oxidation activity of this mineral surface
83 and its catalytic stability. In addition, the binding and transformation mechanisms of organic
84 compounds interacted with laterite surfaces remain unclear.
85 This work aims to develop an effective heterogeneous Fenton process based on the use of a
86 natural catalyst and light source in order to effectively remove emerging contaminants from
87 contaminated water. FLU, an antimicrobial agent belonging to the second generation of
88 synthetic quinolones and frequently used in veterinary medicine (Gothwal and Shashidhar
89 2015), is selected here as a model of emerging pharmaceutical compounds. Due to its
90 continuous release into the environment and its persistence, 2.5-50 ng L^{-1} (Pozo et al. 2006;
91 Tamtam et al. 2008) and 6.9 µg kg^{-1} (Tamtam et al. 2011) of FLU residues have been
92 detected in aquatic environments and in the soil, respectively. To the best of our knowledge,
93 the removal of fluoroquinolone antibiotics using laterite soil as sorbent/catalyst was rarely
94 investigated. Here, the FLU removal was investigated at two pH values (pH 3 as an acidic pH
95 to ensure a high solubility of iron and pH 6.5, closer to near-neutral conditions of real
96 effluents) and with and without UVA irradiation. The influence of laterite loading and initial
97 concentrations of FLU and oxidant (H_2O_2) on the removal efficiency rate was also
98 investigated.
99 Higher concentrations of FLU than those encountered in real contaminated effluents were
100 used in order to test the removal capacity of laterite in heavily loaded contaminated waters,

e.g. multi-components contaminated water. Effect of co-occurring antibiotic on the FLU degradation was also evaluated using norfloxacin (NOR), a fluoroquinolone antibiotic, which can be co-found with FLU in affected environments (Tamtam et al. 2008). The Langmuir and Langmuir–Hinshelwood models were used to describe the surface interactions with FLU in the absence and the presence of oxidant (H_2O_2), respectively. Moreover, possible deactivation of surface sites as well as the catalytic stability of laterite were assessed by conducting sequential oxidation cycles, TOC measurements and solid characterization.

2. Experimental

2.1. Materials

Flumequine (99% purity), norfloxacin (99% purity), hydrogen peroxide (35% w/w), 1,10-phenanthroline (>99% purity), sodium acetate (>99% purity), ferrous ammonium sulfate hexahydrate ($(NH_4)_2Fe(SO_4)_2 \cdot 6H_2O$), 2-propanol ($C_3H_8O$), and chloroform ($CHCl_3$) were provided from Sigma–Aldrich. Solutions were prepared with high-purity water obtained from a Millipore Milli-Q system.

2.2. Laterite soil characterization

Laterite soil was collected from Sinématialy town (9°34'60" N and 5°22'60" W) in the north of Ivory Coast. The sample was grinded and passed through 250 µm sieve. The obtained fraction was washed several times with pure water, and then dried at 50 °C.

In order to determine the crystal structure of natural mineral, sample of laterite (≤ 250 µm) was analyzed by X-ray powder diffraction (XRD). The XRD data were collected with a D8 Bruker diffractometer, equipped with a monochromator and a position-sensitive detector. The XRD peaks (Fig. S1) were attributed to quartz, goethite, hematite, kaolinite and gibbsite. However, the most abundant phases in our sample are quartz, goethite and hematite, which is in agreement with a previous work (Coulibaly et al. 2016). Consistently, the TEM-EDX

indicated a composition of Fe, Al and O (i.e. under oxide forms), together with two major elements Ca and Mg (Fig. S1). More details are given in the supporting information. To determine the metal contents in laterite, elements were analyzed using an inductively coupled plasma atomic emission spectrometer (ICP-AES, Jobin-Yvon JY 70 Type HORIBA) after acid digestion of the sample (Table S1). Potentiometric titrations of the laterite were conducted in thermostated double walled pyrex cell at 293 K in 0.001, 0.01 and 0.1 M NaCl solutions. The pH value of the suspensions was adjusted and kept constant with titrant solutions (HCl or NaOH) at pH 3 or 6.5. The B.E.T. specific surface area and the Point Zero Charge (PZC) of laterite soil were 23 ± 1 m^2 g^{-1} and 6.5 ± 0.3, respectively.

2.3. Photoreactor and photodegradation experiments

All experiments were performed in a 500 mL capacity batch photoreactor (made of borosilicate glass) at room temperature (20 ± 2 °C). The reactor was designed in a column shaped in 34 cm high and 3.8 cm diameter. This setup has an enclosed chamber comprising a reactor; an UVA lamp 24 W (Philips PL-L) placed in the center of the glass cell emitting in a wavelength region 320–400 nm with emission peak centered at λ_{max} = 360 nm, yielding a irradiation intensity of 16 mW cm^{-2} as detected with a UVA Radiometer (VLX- 3W equipped with a sensor CX 365, ALYS Technologies, Switzerland). The solution with catalyst was continuously stirred with a magnetic bar at 180 rpm. The pH of the sample solution was measured by means of VWR instruments 6000 pH-meter. Monitoring of suspension temperature indicated no significant fluctuation (20 ± 2 °C) along the experiment. The UV-visible spectrum of FLU is shown in Figure S2.

Two different experiments were conducted at room temperature. In a first experiment, the suspension of FLU and laterite was stirred in the dark for 4 h to reach the adsorption equilibrium without UVA irradiation and oxidant (H_2O_2). In the second test, FLU, oxidant, and laterite were mixed simultaneously under UVA irradiation. In both experiments, 500 mL

of a FLU solution of known concentration were prepared and the appropriate amount of catalyst was added. In order to keep it constant, the pH of the solution was adjusted by HCl and NaOH (0.1 M). Then, the required volume of H_2O_2 (35% w/w) was added to the solution. At time intervals, 5 mL of the solution were collected and analyzed.

Aqueous organic compound concentrations were determined using a high performance liquid chromatography (Waters 600 Controller) equipped with a reversed-phase C18 column (250 mm×4.6 mm i.d., 5 μm) and UV detector (Waters 2489). The detector was set to 246 nm for FLU and 277 nm for NOR. The mobile phase was mixture of acetonitrile/water (20/80 v/v) containing 0.1% formic acid. The flow rate was set at 1 mL min^{-1} in isocratic mode. Total Organic Carbon (TOC) was determined using a TOC-meter (Shimadzu TOC-VCSH) using 10 mL of solution. Total dissolved iron concentrations were measured by the 1,10-phenantrholine method at 510 nm (Tamura et al. 1974). All these experiments were repeated 2 times and showed a good reproducibility with a standard deviation of 3%.

3. Results and discussion

3.1. Preliminary characterization of removal capacity of the investigated laterite

To characterize the sorption capacity of laterite, adsorption isotherms were determined at two pH values (3 and 6.5) (Fig.1). Preliminary kinetic batch experiments conducted over 24 h showed that equilibrium was achieved within 4 h of reaction time. The experimental isotherm data were best fitted to the equation of Langmuir through linear regression (r^2 = 0.99). The linear form of the Langmuir equation is given by:

$$\frac{C_e}{q_e} = \frac{1}{K_a q_m} + \frac{1}{q_m} C_e \qquad (1)$$

where q_m (μmol m^{-2}) is Langmuir maximum sorbed amount and K_a (L μmol^{-1}) is the Langmuir isotherm constant. The progressive saturation of the surface sites shows that the adsorption followed the Langmuir assumption with a maximum adsorption capacity of 1.40

177 µmol m^{-2} at pH 3 and 1.19 µmol m^{-2} at pH 6.5. As typically encountered for anionic ligands,
178 FLU adsorption was greatest under acidic to circumneutral pH, and lowest under alkaline
179 conditions (See Fig. S3 for distribution of FLU species at various pH values). The K_a values
180 estimated from Langmuir model are 1.95 L μmol^{-1} at pH 3 and 0.37 L μmol^{-1} at pH 6.5.
181 The removal of FLU was then evaluated under different oxidation systems in presence and in
182 absence of laterite (Fig. 2). The heterogeneous process (*i.e.* UVA/H_2O_2/Laterite) showed the
183 best removal performance at both pH values, 77% and 62% of removal at pH 3 and 6.5,
184 respectively. In both experiments, the direct photolysis is less than 12%. To account for the
185 sorption on laterite, desorption tests (adding NaOH to have pH 11) were performed and total
186 amounts of FLU in aqueous phase were plotted against time (Fig. 2). The amounts of
187 degraded FLU lied at 56% at pH 3, and 43% at pH 6.5 and after 420 min of reaction time. It is
188 worth noting that pre-equilibration of FLU with laterite suspension for 4 h in the dark before
189 irradiation did not significantly change the kinetics behavior (Fig.S4). TOC measurements
190 over 540 min confirmed the oxidative degradation in UVA/H_2O_2/Laterite system, whereas
191 45% and 33% of mineralization was achieved at pH 3 and 6.5, respectively. As explained
192 below, optimization of experimental parameters improved the FLU degradation up to 94%,
193 and mineralization up to 72%.
194
195 The higher degradation performance at pH 3 may result from (i) changes in surface
196 interactions between FLU and laterite as more adsorption was observed at pH 3, (ii) high
197 formation rate of radical species at acidic pH (Buxton et al. 1988) and/or (iii) possible
198 leaching of Fe from laterite surfaces contributing to a homogeneous Fenton reaction. The
199 latter was excluded since the amount of iron leaching was found very low (< 6 $\mu g.L^{-1}$) even if
200 it is relatively higher at acidic pH than at pH 6.5 (Fig. S5). The possible release of trace

elements such as Cr, Cu, Co, Ni and Zn was also checked by ICP/AES, which indicated that these elements were under quantification limits under our experimental conditions.

We note an increase of FLU degradation in UVA/H_2O_2/Laterite compared to UVA/H_2O_2 system. This improvement could be attributed to the higher generation of active species, e.g. hydroxyl radicals and iron ferrous (Fe^{II}) (Martínez et al. 2007; Gonzalez-Olmos et al. 2012; Minella et al. 2014). First, direct photolysis of H_2O_2 under UVA irradiation may generate highly oxidizing species (*i.e.* •OH radicals). Moreover, the UVA irradiation may also enhance the heterogeneous Fenton activity on the surface, by promoting the photo-assisted reduction of Fe^{III} to Fe^{II}, which subsequently reacts with H_2O_2 generating •OH radicals. Therefore, addition of H_2O_2 led to an acceleration of reaction rate, as compared to the UVA/Laterite system, further confirming the synergetic effect of laterite and H_2O_2.

3.3. Optimization of operating conditions

The influences of H_2O_2 concentration, laterite dosage and initial concentration on the removal of FLU were investigated at pH 3 and 6.5. The experiments, which were repeated 2 times, showed a good reproducibility with a 5% of averaged standard deviation.

3.3.1. Effect of H_2O_2 concentration

Removal kinetics of FLU were determined at a wide range of H_2O_2 concentration (1 - 9 mmol L^{-1}) and two pH values (3 and 6.5). The degradation of organic compounds by $HO^{\cdot}$ is typically described as a second-order reaction [1-6]:

$$\frac{d[FLU]}{dt} = -k[FLU][HO^{\cdot}] \quad (2)$$

where [$HO^{\cdot}$] is steady-state concentration of hydroxyl radical, [FLU] is concentration of FLU in water, k is the second-order rate constant, and t is the reaction time. By assuming that $HO^{\cdot}$

instantaneous concentration is constant, the kinetics of degradation of FLU in water can be described according to the pseudo-first-order equation as given below:

$$[FLU]_t = [FLU]_0 \exp(-k_{app} t) \quad (3)$$

where k_{app} is the pseudo-first-order apparent rate constant (min^{-1}). k_{app} (min^{-1}) obtained by linear regression of ln (C_t/C_o) versus time *t*, was plotted against H_2O_2 concentration. The k_{app} constants were higher at pH 3 than pH 6.5. Since the degradation of FLU solution is directly related to the concentration of hydrogen peroxide and formation of radicals, the removal kinetic of FLU was enhanced when the H_2O_2 concentration increased from 1 to 4 mmol L^{-1}. However, a decrease in k_{app} was observed at higher H_2O_2 concentrations (Fig. 3), thereby suggesting scavenging effects of radicals by hydrogen peroxide ($k_{H2O2/HO^{\cdot}} = 2.7 \times 10^7\ M^{-1}\ s^{-1}$) (Mechakra et al. 2016) and/or recombination of radicals (Buxton et al. 1988; Litter et al. 2017). At much higher H_2O_2 concentration, there is a competitive reaction between FLU and H_2O_2 towards the reaction with ROS.

3.3.2. Effect of laterite dosage

The pseudo-first-order apparent rate constants (k_{app} (min^{-1})) were determined as previously explained, and plotted against laterite loading (0.5 to 4 g L^{-1}) in Figure 4. As for previous experiments, the observed pseudo-first order rate constant firstly increased with laterite loading increasing and then reduced. This phenomenon can be explained by screening effects occurring at high loading of solid in aqueous suspension, as previously reported for heterogeneous photo-Fenton reactions (Bohu et al. 2008; Mechakra et al. 2016). In addition, the generated radicals can be scavenged by metal oxide surfaces ($k_{oxide/HO^{\cdot}} = 8 \times 10^{11}$ (g mL^{-1})$^{-1}$ s^{-1}) (Miller and Valentine 1999).

249 It is interesting to note that the optimal laterite loading of FLU removal is around 1 g L^{-1}
250 regardless of the tested pH (k_{app} = 6.4 x10^{-3} ± 0.0003 min^{-1} and 4.6 x10^{-3} ± 0.0003 min^{-1} at pH
251 3 and pH 6.5, respectively).

252
253 **3.3.3. Effect of initial flumequine concentration**

254 The pseudo first-order rate constants (k_{app}) at various initial concentrations of FLU were
255 determined with the optimum conditions for laterite loading and oxidant concentration (Fig.
256 5). There is a decrease of k_{app} from 1.87x10^{-2} ± 0.0003 to 6.2 x10^{-3} ± 0.0003 min^{-1} at pH 3 and
257 from 9.4x10^{-3} ± 0.0003 to 4.1 x10^{-3} ± 0.0003 min^{-1} at pH 6.5 when FLU concentration
258 increased from 19 to 77 µmol L^{-1}. This expected phenomenon can be explained by the
259 competition of species (here FLU and H_2O_2) with each other for interactions with a fixed
260 number of active sites on solid surfaces. At higher FLU concentration, adsorption may occupy
261 a greater number of Fe^{III}-sites, which become unavailable to generate Fe^{II} upon irradiation
262 and/or interact with H_2O_2. This is consistent with previous works where photon absorption by
263 catalyst or photo-assisted reduction of surface sites to trigger the oxidation reaction is
264 considered as the rate-limiting step (Avetta et al. 2015). Furthermore, higher FLU
265 concentrations may lead to a decrease of photons entering into solution thereby lowering the
266 performance of photo-assisted Fenton reaction, as previously reported (Rivas et al. 2015).
267 The Langmuir-Hinshelwood model that is widely used in heterogeneous catalysis was tested
268 here (Turchi et al. 1990) to describe the oxidation process at the oxide surface. This
269 Langmuir-Hinshelwood model can be expressed as:

270 $$k_{app} = \frac{k_{\text{int}} K_s}{1 + K_s C_0} \quad (4)$$

271 and linear expression :

272 $$\frac{1}{k_{app}} = \frac{C_0}{k_{\text{int}}} + \frac{1}{k_{\text{int}} K_s} \quad (5)$$

where k_{app} is the initial pseudo-first-order rate constant (min^{-1}), k_{int} is the intrinsic reaction rate constant ($\mu mol\ L^{-1}\ min^{-1}$), and K_s is the adsorption constant of FLU over laterite surfaces ($L\ \mu mol^{-1}$). The linear correlations ($r^2 = 0.99$) between $1/k_{app}$ and C_o are good at both pH (3 and 6.5), indicating that surface reactions of FLU including sorption and oxidation played a key role in determining the rate of the whole reaction. The values of k_{int} and K_s obtained are 0.51 $\mu mol\ L^{-1}\ min^{-1}$ and 0.12 $L\ \mu mol^{-1}$ at pH 3 and 0.33 $\mu mol\ L^{-1}\ min^{-1}$ and 0.06 $L\ \mu mol^{-1}$ at pH 6.5. The K_s values estimated from L-H model are lower than the constants determined in the absence of oxidant by Langmuir model (1.95 $L\ \mu mol^{-1}$ at pH 3 and 0.37 $L\ \mu mol^{-1}$ at pH 6.5), underscoring competition effects between species at laterite surfaces.

3.4. Implication of radical species in the degradation process

Different ROS may be formed during heterogeneous photo-Fenton reaction such as $^{\bullet}OH$ and/or $HO_2^{\bullet}/O_2^{\bullet-}$ (Martínez et al. 2005; Xue et al. 2009). In order to better understand the process involved in the degradation of FLU, 2-propanol was used as scavenger as it can react with $^{\bullet}OH$ radical with relatively high reaction rate constant ($k = 1.9 \times 10^9\ M^{-1}\ s^{-1}$). Chloroform was also used as the scavenger of $HO_2^{\bullet}/O_2^{\bullet-}$ radical due to its relatively high reaction rate constant with hydrated electron ($k = 3.0 \times 10^{10}\ M^{-1}\ s^{-1}$) and relatively low reaction rate constant with $^{\bullet}OH$ radical ($k = 7.4 \times 10^6\ M^{-1}\ s^{-1}$) (Anbar and Neta, 1967). Because the pKa of $HO_2^{\bullet}/O_2^{\bullet-}$ is 4.8, the hydroperoxide anion $HO_2^{\bullet}$ is the predominant form at pH 3 while the superoxide anion $O_2^{\bullet-}$ is preponderant at pH 6.5 (Bielski et al. 1985).

First, 10 $mmol\ L^{-1}$ of 2-propanol fully inhibited the FLU degradation (only oxidation is considered here as the total FLU concentration was plotted versus time, Fig. S6), suggesting that the $^{\bullet}OH$ radical was by far the dominant species in the FLU degradation at pH 3. At pH 6.5, 2-propanol did not fully stopped the FLU degradation, while the effect of chloroform is

more pronounced than at pH 3, suggesting that hydroxyl radicals still predominantly degrade FLU, but to a lower extent.

In the presence of 10 mmol L^{-1} of chloroform, the percentage of removed FLU fell down from 50% in the absence of chloroform to around 37% at pH 6.5, suggesting that $O_2^{\bullet-}$ radicals may play a role in FLU degradation (Fig. S6). $O_2^{\bullet-}$ can promote the formation of $^{\bullet}OH$ through the reduction of Fe^{III} to Fe^{II} (Bielski et al. 1985; Lin and Gurol 1998):

$$\equiv Fe^{III} + O_2^{\bullet-} \longrightarrow \equiv Fe^{II} + O_2 \qquad k = 1.2 \times 10^6\ M^{-1}\ s^{-1} \tag{6}$$

Nevertheless, the use of 2-propanol at both tested pH led to relatively high inhibition of degradation, confirming that the oxidation of FLU is mainly due to $^{\bullet}OH$ radicals.

3.5. Effect of co-occurring antibiotic on the FLU degradation

The influence of presence of co-solute on the degradation efficiency of FLU was evaluated with the optimum conditions for laterite loading and oxidant concentration and at two pH values (3 and 6.5). The photo-assisted degradations of FLU ($[k_{FLU, \bullet OH}] = 8.26 \times 10^9\ M^{-1}\ s^{-1}$ at pH 7 (Santoke et al. 2009)) and NOR ($[k_{NOR, \bullet OH}] = 6.18 \times 10^9\ M^{-1}\ s^{-1}$ at pH 7 (An et al. 2010)) were evaluated in separate system (FLU or NOR) and binary system (an equimolar mixture of FLU and NOR) (Fig.6).

Firstly, the degradation of each compound in the mixture decreased with respect to the single system, probably due to competition of compounds for reaction with hydroxyl radicals.

As an attempt to better understand the competition effect, the percentage of the hydroxyl radical ($^{\bullet}OH$) reacted with FLU can be estimated using the following equation (Huang et al. 2013):

$$R_{Flu} = \frac{k_{^{\bullet}OH, Flu}\,[Flu]_o}{k_{^{\bullet}OH, Flu}\,[Flu]_o + k_{^{\bullet}OH, Nor}\,[Nor]_o + k_{^{\bullet}OH, H_2O_2}\,[H_2O_2]_o} \tag{7}$$

Where [$k_{^{\bullet}OH,\ FLU}$], [$k_{^{\bullet}OH,\ NOR}$] and [$k_{^{\bullet}OH,\ H_2O_2}$] are the second-order rate constants between $^{\bullet}OH$ and FLU, NOR and hydrogen peroxide. $k_{^{\bullet}OH,\ H_2O_2}$= 2.7×10^7 M^{-1} s^{-1} (Buxton et al. 1988). $[FLU]_0$, $[NOR]_0$ and $[H_2O_2]_0$ were their initial concentrations. The same equation can be used to determine the percentage of the hydroxyl radical ($^{\bullet}OH$) reacted with NOR, by replacing $[FLU]_0$ by $[NOR]_0$ in the numerator of eq. 12. Since the reaction rate constants of FLU ([$k_{FLU,^{\bullet}OH}$] = 8.26×10^9 M^{-1} s^{-1}) (Santoke et al. 2009) and of NOR ([$k_{NOR,\ ^{\bullet}OH}$] = 6.18×10^9 M^{-1} s^{-1}) (An et al. 2010) with the hydroxyl radical are relatively close, 41% and 31% of $^{\bullet}OH$ reacted with FLU and NOR, respectively. It is worth noting that these reaction rate constants were determined at pH buffered to 7 (i.e. $pKa_1 < pH < pKa_2$ for NOR where the zwitterionic form is the predominant species, and $pH > pK_a$ for FLU where the anionic form is predominant), which is different from the working pH value (6.5 ± 0.1) in the present study. Nevertheless, we can conclude that the degradation of each compound (FLU or NOR) is not considerably affected by the presence of the other, underscoring potential benefits of the investigated process in the treatment of multi-components contaminated systems.

3.6. Stability and reusability of laterite

The reusability of catalyst is a critical parameter, from an economical point of view, for its usage in large scale reactors (Nidheesh 2015). The reusability of laterite has been evaluated in successive oxidation cycles, with the above-mentioned optimum conditions and at two pH conditions (Fig. 7). At the end of the oxidation process, the solid is easily removed from the reactor, washed with ultra-pure water, and dried at 50°C overnight, and then used for next experiment. The degradation using the recovered catalyst showed a slight difference with the first oxidation cycle, suggesting that the catalytic activity kept constant after five cycles of oxidation reaction. The removal rates of FLU were about 6.4×10^{-3} min^{-1} at pH 3 and 4.4×10^{-3} min^{-1} at pH 6.5, whereas percentage efficiencies lied at 94 ± 2% and 70 ± 2%, respectively.

The excellent stability of UVA/H_2O_2/Laterite system was then confirmed through TOC measurements at the end of each oxidation cycle. 72 ± 4% of mineralization was achieved at pH 3 and 50 ± 4% at pH 6.5, and this value remains constant even after 5 oxidation cycles. The dissolved iron concentration measurements showed a very low release of Fe from laterite surfaces (less than 2 wt.% of total Fe initially present in laterite). In addition, XRD diffractogram recorded at the end of oxidation reaction was found to be quite similar with that recorded before reaction (Fig. S1). The excellent stability of the catalytic activity could be, therefore, attributed to the very low iron leaching during oxidation cycles and to the structural stability of the solid.

4. Conclusion

We have notably demonstrated that laterite can be effectively used for the removal of flumequine under UVA irradiation and at two pH values 3 and 6.5. The photo-assisted Fenton oxidation using laterite as iron source is dependent on H_2O_2 dose, laterite loading and initial concentration of FLU. The degradation rate firstly increased with the dosage of H_2O_2 or with laterite loading, reached an optimum value and then decreased. The occurrence of these optimums values could be explained by the parasite's scavenging reactions and/or light-screening effects. The apparent heterogeneous reaction rate is dominated by the rate of intrinsic surface chemical reactions including sorption and light-induced reduction of Fe^{III}, which are crucial to enhance the oxidation reaction. The laterite-promoted degradation of FLU is not dramatically affected by the presence of NOR, which can be co-found in affected environmental systems. The laterite can be re-used for several oxidation cycles without structural changes or deactivation of surface sites. This environmentally friendly remediation technology may appear as a promising way for water treatment in developing countries, using

a low cost natural catalyst and solar light for the removal of fluoroquinolone antibiotics from multi-contaminated waters.

Acknowledgements

This work was supported by a bilateral governmental program, Ivory Cost (Contract C2D) and Campus France. We gratefully acknowledge Dr. M. Pasturel (Rennes University) for XRD analysis and Dr. S. Rtimi (EPFL, Lausanne) for TEM analysis.

Appendix A. Supplementary data

Supplementary data associated with this article can be found, in the online version.

References

An T, Yang H, Song W, Li G, Luo H, Cooper WJ (2010) Mechanistic considerations for the advanced oxidation treatment of fluoroquinolone pharmaceutical compounds using TiO_2 heterogeneous catalysis. J Phys Chem A 114: 2569-2575. doi: 10.1021/jp911349y

Anbar M, Neta P (1967) A Compilation of Specific Bimolecular Rate Constants for the Reactions of Hydrated Electrons, Hydrogen Atoms and Hydroxyl Radicals with Inorganic and Organic Compounds in Aqueous Solution. Inter J Appl Rad Isot 18: 493-523. doi :10.1016/0020-708X(67)90115-9

Anipsitakis GP, Dionysiou DD (2004) Radical generation by the interaction of transition metals with common oxidants. Environ Sci Technol 38: 3705-3712. doi**:** 10.1021/es035121o

Avetta P, Pensato A, Minella M, Malandrino M, Maurino V, Minero C (2015) Activation of persulfate by irradiated magnetite: implications for the degradation of phenol under heterogeneous photo-Fenton-like conditions. Environ Sci Technol 49(2): 1043-1050. doi: 10.1021/es503741d

Bielski BHJ, Cabelli DE, Arudi RL, Ross AB (1985) Reactivity of $HO_2^{\bullet}/O_2^{\bullet-}$ Radicals in Aqueous Solution. J Phys Chem Ref Data 14: 1041-1100. doi :10.1063/1.555739

Bohu M, Yediler A, Siminiceanu I, Schulte-Hostede S (2008) Degradation studies of ciprofloxacin on a pillared iron catalyst. Appl Catal B: Environ 83: 15-23. doi :10.1016/j.apcatb.2008.01.029

Buxton GV, Greenstock CL, Helman WP, Ross AB (1988) Critical review of rateconstants for reactions of hydrated electrons, hydrogen atoms and hydroxylradicals ($^{\bullet}OH/O^{\bullet-}$) in aqueous solution. J Phys Chem Ref Data 17: 513–886. doi :10.1063/1.555805

Coulibaly LS, Akpo SK, Yvon J, Coulibaly L (2016) Fourier transform infra-red (FTIR) spectroscopy investigation, dose effect, kinetics and adsorption capacity of phosphate from aqueous solution onto laterite and sandstone. J Environ Manag 183: 1032-1040. doi :10.1016/j.jenvman.2016.09.061

Dias FF, Oliveira AAS, Arcanjo AP, Moura FCC, Pacheco JGA (2016) Residue-based iron catalyst for the degradation of textile dye via heterogeneous photo-Fenton. Appl Catal B: Environ 186: 136–142. doi :10.1016/j.apcatb.2015.12.049

Garrido-Ramirez EG, Theng BKG, Mora ML (2010) Clays and oxide minerals as catalysts and nanocatalysts in Fenton-like reactions-A review. Appl Clay Sci 47: 182-192. doi :10.1016/j.clay.2009.11.044

Ghauch A, Baydoun H, Dermesropian P (2011) Degradation of aqueous carbamazepine in ultrasonic/Fe_0/H_2O_2 systems. Chem Eng J 172 (1): 18-27. doi :10.1016/j.cej.2011.04.002

Gonzalez-Olmos R, Martin MJ, Georgi A, Kopinke F-D, Oller I, Malato S (2012) Fe-zeolites as heterogeneous catalysts in solar Fenton-like reactions at neutral pH. Appl Catal B: Environ 125: 51-58. doi :10.1016/j.apcatb.2012.05.022

Gonzalez-Olmos R, Roland U, Toufar H, Kopinke F-D, Georgi A (2009) Fe-zeolites as catalysts for chemical oxidation of MTBE in water with H_2O_2. Appl Catal B: Environ 89: 356-364. doi.org/10.1016/j.apcatb.2008.12.014

Gothwal R, Shashidhar T (2015) Antibiotic Pollution in the Environment: A Review. Clean-Soil, Air, Water 43(4): 479-489. doi: 10.1002/clen.201300989

Guo L, Chen F, Fan X, Cai W, Zhang J (2010) S-doped α-Fe_2O_3 as a highly active heterogeneous Fenton-like catalyst towards the degradation of acid orange 7 and phenol. Appl Catal B: Environ 96: 162-168. doi :10.1016/j.apcatb.2010.02.015

Herney-Ramirez J, Vicente MA, Madeira LM (2010) Heterogeneous photo-Fenton oxidation with pillared clay-based catalysts for wastewater treatment: A review. Appl Catal B: Environ 98: 10 -26. doi : 10.1016/j.apcatb.2010.05.004

Huang W, Brigante M, Wu F, Mousty C, Hanna K, Mailhot G (2013) Assessment of the Fe(III)-EDDS complex in Fenton-Like processes: From the radical formation to the degradation of Bisphenol A. Environ Sci Technol 47: 1952-1959. doi: 10.1021/es304502y

Karale R, Manu B, Shrihari S (2013) Catalytic use of laterite iron for degradation of 2 aminopyridine using advanced oxidation processes. Inter J Sci Eng Res 4: 207-210.

Khataee A, Salahpour F, Fathinia M, Seyyedi B, Vahid B (2015) Iron rich laterite soil with mesoporous structure for heterogeneous Fenton-like degradation of an azo dye under visible light. J Ind Eng Chem 26: 129 -135. doi :10.1016/j.apcatb.2010.05.004

Kwan WP, Voelker BM (2003) Rates of hydroxyl radical generation and organic compounds oxidation in mineral-catalyzed Fenton-like systems. Environ Sci Technol 37: 1150 - 1158. doi: 10.1021/es020874g

Lan H, Wang A, Liu R, Liu H, Qu J (2015) Heterogeneous photo-Fenton degradation of acid red B over Fe_2O_3 supported on activated carbon fiber. J Hazard Mater 285: 167-172. doi :10.1016/j.jhazmat.2014.10.057

Lin S-S, Gurol MD (1998) Catalytic Decomposition of Hydrogen Peroxide on Iron Oxide: Kinetics, Mechanism, and Implications. Environ Sci Technol 32 (10): 1417-1423. doi: 10.1021/es970648k

Lin S-S, Gurol MD (1998) Catalytic Decomposition of Hydrogen Peroxide on Iron Oxide: Kinetics, Mechanism, and Implications. Environ Sci Technol 32: 1417-1423. doi: 10.1021/es970648k

Litter MI, Candal RJ, Meichtry JM (2017) Advanced Oxidation Technologies: Sustainable Solutions for Environmental Treatments, CRC Press ISBN 9781138072886, 350p.

Martinez F, Calleja G, Melero JA, Molina R (2005) Heterogeneous photo-Fenton degradation of phenolic aqueous solutions over iron-containing SBA-15 catalyst. Appl Catal B: Environ 60: 181-190. doi :10.1016/j.apcatb.2005.03.004

Martínez F, Calleja G, Melero JA, Molina R (2007) Iron species incorporated over different silica supports for the heterogeneous photo-Fenton oxidation of phenol. Appl Catal B: Environ 70: 452-460. doi :10.1016/j.apcatb.2005.10.034

Matta R, Hanna K, Chiron S (2007) Fenton-like oxidation of 2, 4, 6-trinitrotoluene using different iron minerals. Sci Total Environ 385(1): 242-251. doi:10.1016/j.scitotenv.2007.06.030

Mechakra H, Sehili T, Kribeche MA, Ayachi AA, Rossignol S, George C (2016) Use of natural iron oxide as heterogeneous catalyst in photo-Fenton-like oxidation of chlorophenylurea herbicide in aqueous solution: Reaction monitoring and degradation pathways. J Photochem Photobiol A: Chem 317: 140-150. doi :10.1016/j.jphotochem.2015.11.019

Miller CM, Valentine RL (1999) Mechanistic studies of surface catalyzed H_2O_2 decomposition and contaminant degradation in the presence of sand. Water Res 33(12): 2805-2816. doi :10.1016/S0043-1354(98)00500-4

Minella M, Marchetti G, De Laurentiis E, Malandrino M, Maurino V, Minero C, Vione D, Hanna K (2014) Photo-Fenton oxidation of phenol with magnetite as iron source, Appl. Catal. B: Environ 154(155): 102-109. doi :10.1016/j.apcatb.2014.02.006

Nidheesh PV (2015) Heterogeneous Fenton catalysts for the abatement of organic pollutants from aqueous solution: a review. RSC Adv 5: 40552 – 40577. doi:10.1039/C5RA02023A

Pignatello JJ, Oliveros E, MacKay A (2006) Advanced oxidation processes for organic contaminant destruction based on the Fenton reaction and related chemistry. Crit. Rev. Environ. Sci Technol 36 (1): 1– 84. doi :10.1080/10643380500326564

Pozo OJ, Guerrero C, Sancho JV, Ibańez M, Pitarch E, Hogendoorn E, Hernández F (2006) Efficient approach for the reliable quantification and confirmation of antibiotics in water using on-line solid-phase extraction liquid chromatography/tandem mass spectrometry. J Chromatogr A 1103: 83-93. doi :10.1016/j.chroma.2005.10.073

Rivas G, Carra I, Sánchez JLG, López JLC, Malato S, Pérez JAS (2015) Modelling of the operation of raceway pond reactors for micropollutant removal by solar photo-Fenton as a function of photon absorption. Appl Catal B: Environ 178: 210-217. doi.10.1016/j.apcatb.2014.09.015

Ruales-Lonfat C, Barona JF, Sienkiewicz A, Bensimon M, Vélez-Colmenares J, Benítez N, Pulgarín C (2015) Iron oxides semiconductors are efficients for solar water disinfection: A comparison with photo-Fenton processes at neutral pH. Appl Catal B: Environ 166-167: 497-508. doi.10.1016/j.apcatb.2014.12.007

Santoke H, Song W, Cooper WJ, Greaves J, Miller GE (2009) Free-radicals-Induced oxidative and reductive degradation of fluoroquinolone pharmaceuticals: Kinetic studies and degradation mechanism. J Phys Chem A 113: 7846-7851. doi: 10.1021/jp9029453

Tamtam F, Mercier F, Le Bot B, Eurin J, Dinh QT, Clément M, Chevreuil M (2008) Occurrence and fate of antibiotics in the Seine River in various hydrological conditions. Sci Total Environ 393: 84-95. doi :10.1016/j.scitotenv.2007.12.009

Tamtam F, Van Oort F, Le Bot B, Dinh T, Mompelat S, Chevreuil M, Lamy I, Thiry M, (2011) Assessing the fate of antibiotic contaminants in metal contaminated soils four years after cessation of long-term waste water irrigation. Sci Total Environ 409: 540-547. doi :10.1016/j.scitotenv.2010.10.033

Tamura H, Goto K, Yotsuyanagi T, Nagayama M (1974) Spectrophotometric determination of iron (II) with 1,10-phenanthroline in the presence of large amounts of iron(III). Talanta 21: 314-318. doi :10.1016/0039-9140(74)80012-3

Teel AL, Watts RJ (2002) Degradation of carbon tetrachloride by modified Fenton's reagent, J Hazard Mater B 94: 179-189. doi :10.1016/S0304-3894(02)00068-7

Turchi GS, Ollis DF (1990) Photocatalytic degradation of organic water contaminants: Mechanisms involving hydroxyl radical attack. J Catal 122: 178-192. doi :10.1016/0021-9517(90)90269-P

Wang Y, Gao Y, Chen L, Zhang H (2015) Goethite as an efficient heterogeneous Fenton catalyst for the degradation of methyl orange. Catal Today 252: 107-112. doi:10.1016/j.cattod.2015.01.012

Xue X, Hanna K, Abdelmoula M, Deng N (2009) Adsorption and oxidation of PCP on the surface of magnetite: Kinetic experiments and spectroscopic investigations. Appl Catal B: Environ 89: 432-440. doi.org/10.1016/j.apcatb.2008.12.024

Capture Figures

Fig.1. Adsorption isotherms of flumequine (FLU) on laterite at pH 3 and 6.5: $[FLU]_o$ = 19 -77 µmol.L^{-1}; [Laterite] = 1 g L^{-1}. Solid lines represent the Langmuir model.

Fig.2. Kinetics of flumequine (FLU) removal for various oxidation processes at pH 3 and pH 6.5: $[FLU]_o$ = 77 µmol L^{-1}; $[H_2O_2]$ = 1 mmol L^{-1}; [Laterite] = 1g L^{-1}; $[FLU]_{aq}$ = aqueous (residual) concentration of flumequine. $[FLU]_{tot}$ = total concentration of flumequine representing both aqueous (residual) concentration and adsorbed concentration obtained after desorption. Solid lines represent the pseudo-first order model.

Fig.3. Effect of H_2O_2 concentration on flumequine (FLU) removal by heterogeneous photo-Fenton process at pH 3 and pH 6.5: $[FLU]_o$ = 77 µmol L^{-1}; [Laterite] = 1g L^{-1}; UVA irradiation; reaction time = 420 min.

Fig.4. Effect of laterite dosage on flumequine (FLU) removal by heterogeneous photo-Fenton process at pH 3 and pH 6.5: $[FLU]_o$ = 77 µmol L^{-1}; UVA irradiation; $[H_2O_2]$ = 4 mmol L^{-1}; reaction time = 420 min.

Fig.5. kinetic rate constants of flumequine (FLU) versus initial concentration of flumequine in heterogeneous photo-Fenton processes at pH 3 and pH 6.5: $[FLU]_o$ = 19-77 µmol L^{-1}; [laterite] = 1g L^{-1}; $[H_2O_2]$ = 4 mmol L^{-1}; UVA irradiation ; reaction time = 420 min.

Fig.6. Total concentration of flumequine (FLU) and norfloxacin (NOR) degraded versus time in single and binary systems in the heterogeneous photo-Fenton process at two pH values (3 and 6.5): $[FLU]_o$ = $[NOR]_o$ = 19 µmol L^{-1}; [laterite] = 1 g L^{-1}; $[H_2O_2]$ = 4 mmol L^{-1}; UVA irradiation; reaction time = 300 min.

Fig.7. Reusability cycles of laterite in the heterogeneous photo-Fenton process at pH 3 and pH 6.5: $[FLU]_o$ = 77 µmol L^{-1}; [laterite] = 1 g L^{-1}; $[H_2O_2]$ = 4 mmol L^{-1}; UVA irradiation; reaction time = 420 min. Solid line represents pseudo-first order kinetic model.

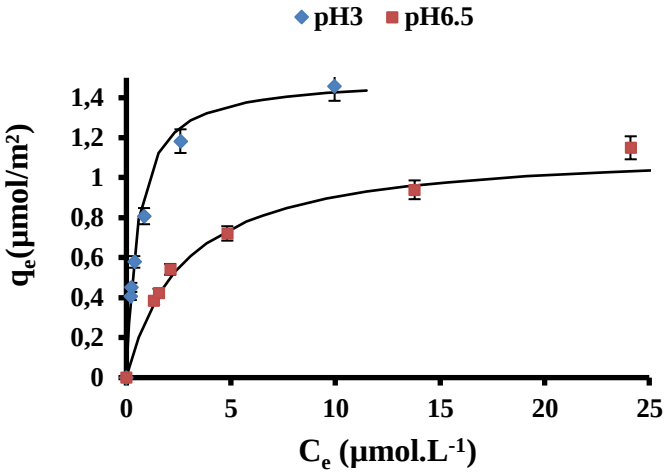

Fig. 1

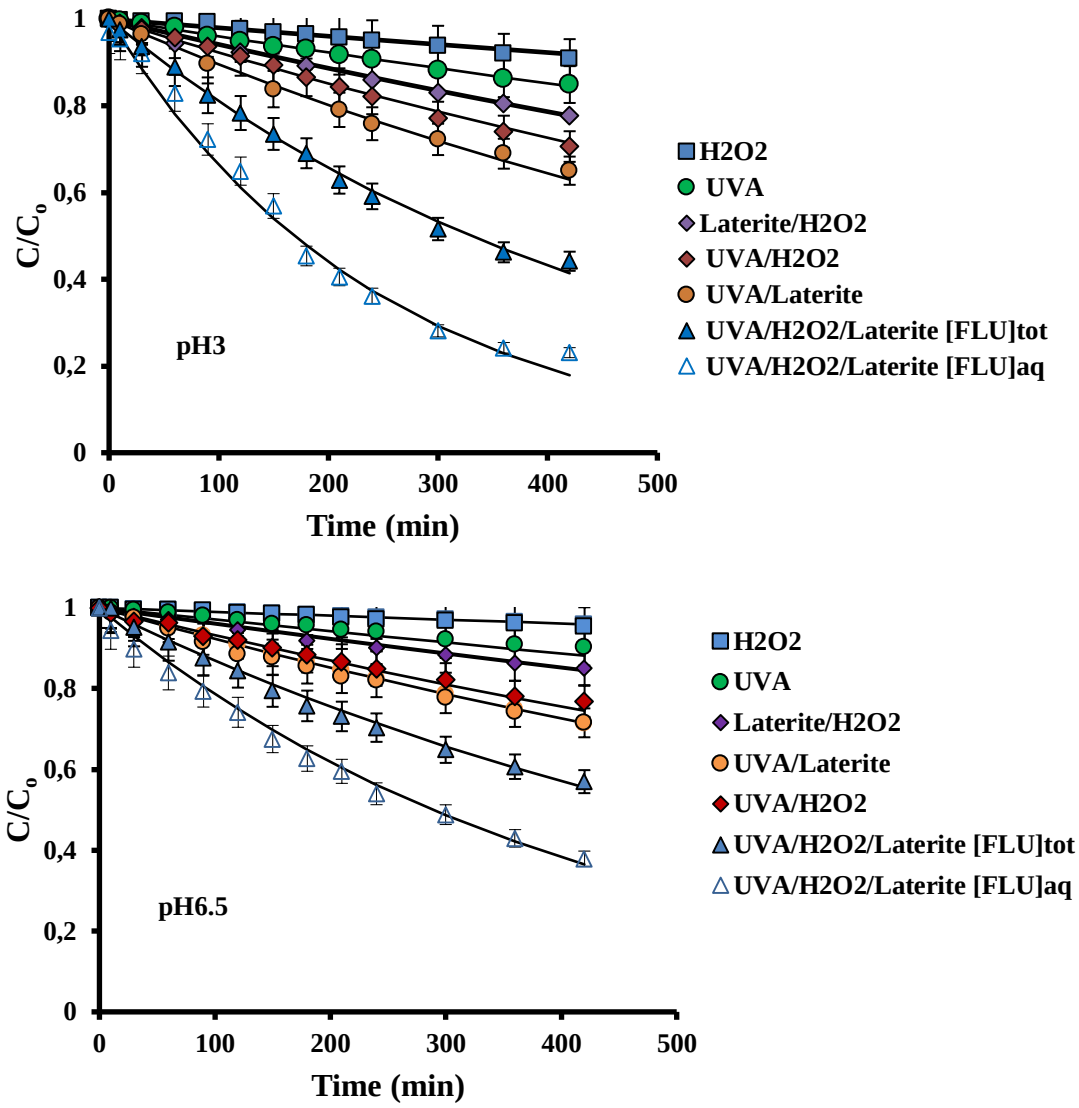
C/C$_o$
pH3
Time (min)
H2O2
UVA
Laterite/H2O2
UVA/H2O2
UVA/Laterite
UVA/H2O2/Laterite [FLU]tot
UVA/H2O2/Laterite [FLU]aq
pH6.5
Time (min)

Fig. 2

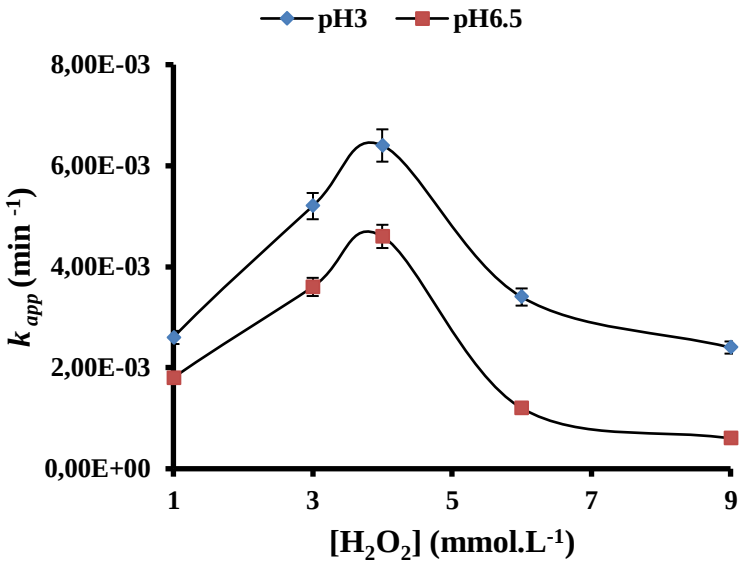
pH3
pH6.5
8,00E-03
6,00E-03
4,00E-03
2,00E-03
0,00E+00
k_{app} (min $^{-1}$)
1
3
5
7
9
[H_2O_2] (mmol.L^{-1})

Fig. 3

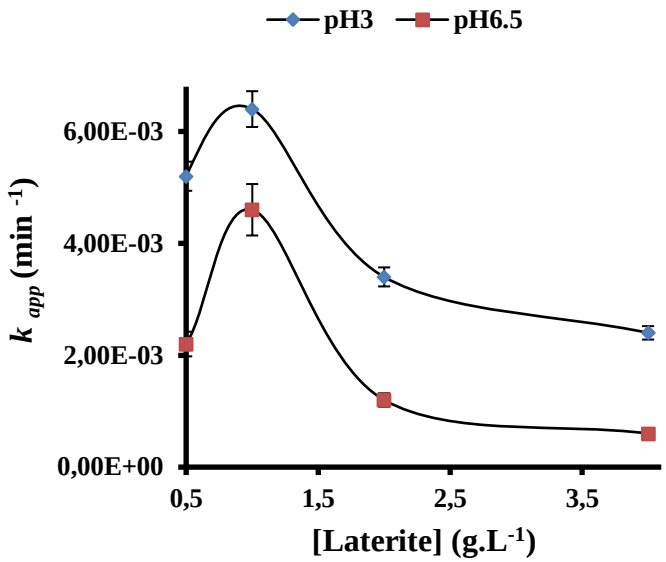
pH3
pH6.5
6,00E-03
4,00E-03
2,00E-03
0,00E+00
k_{app} (min^{-1})
0,5
1,5
2,5
3,5
[Laterite] (g.L^{-1})

Fig. 4

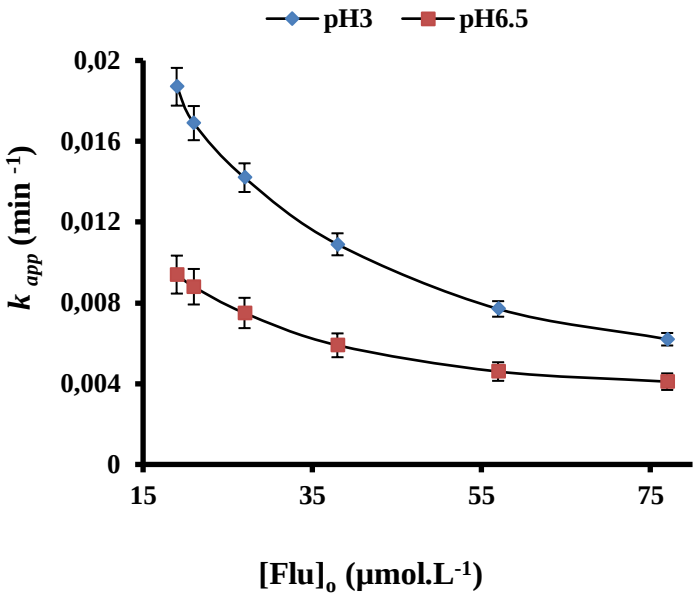
pH3
pH6.5
0,02
0,016
0,012
0,008
0,004
0
15
35
55
75
k_{app} (min^{-1})
[Flu]$_o$ (µmol.L^{-1})

Fig. 5

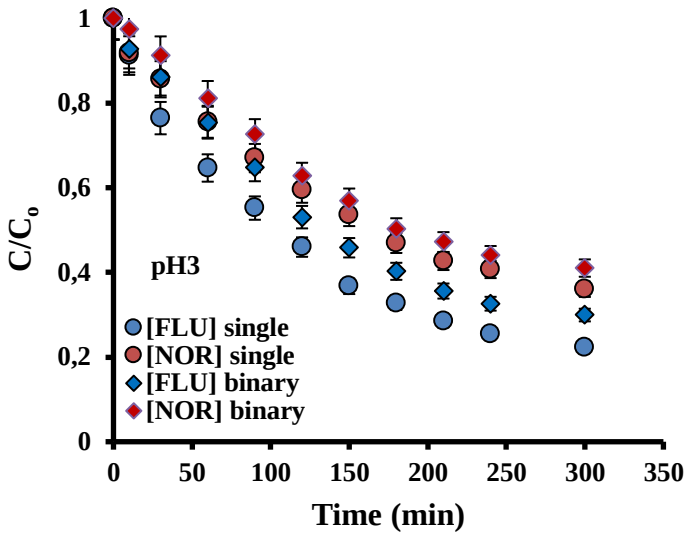
C/C$_o$
pH3
[FLU] single
[NOR] single
[FLU] binary
[NOR] binary
Time (min)

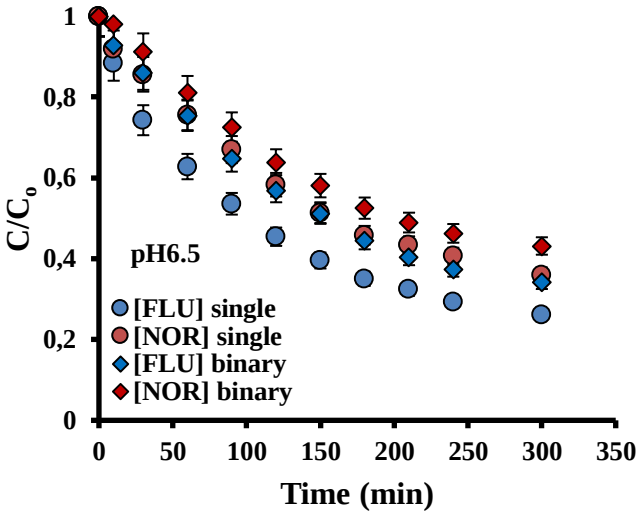
C/C$_o$
pH6.5
[FLU] single
[NOR] single
[FLU] binary
[NOR] binary
Time (min)

Fig. 6

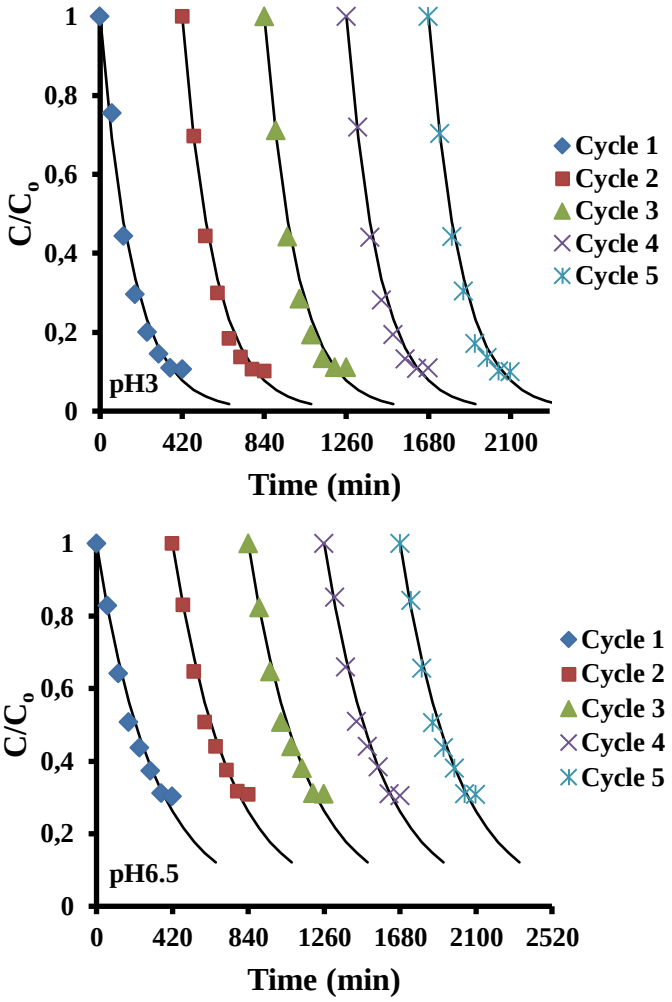
1
0,8
0,6
0,4
0,2
0
C/C$_o$
pH3
0
420
840
1260
1680
2100
Time (min)
Cycle 1
Cycle 2
Cycle 3
Cycle 4
Cycle 5
1
0,8
0,6
0,4
0,2
0
C/C$_o$
pH6.5
0
420
840
1260
1680
2100
2520
Time (min)
Cycle 1
Cycle 2
Cycle 3
Cycle 4
Cycle 5

Fig. 7